Acta Pharmacologica Sinica (2013) 34: 1093–1100
 1671-4083/13 $32.00
www.nature.com/aps

Original Article

Fluopsin C induces oncosis of human breast adenocarcinoma cells

Li-sha MA[1, #], Chang-you JIANG[1, #], Min CUI[1, 2], Rong LU[1], Shan-shan LIU[1, 2], Bei-bei ZHENG[1], Lin LI[1], Xia LI[1, 2, *]

[1]*School of Ocean, Shandong University, Weihai 264209, China;* [2]*School of Pharmaceutical Sciences, Shandong University, Ji-nan 250012, China*

Aim: Fluopsin C, an antibiotic isolated from *Pseudomonas jinanesis*, has shown antitumor effects on several cancer cell lines. In the current study, the oncotic cell death induced by fluopsin C was investigated in human breast adenocarcinoma cells *in vitro*.
Methods: Human breast adenocarcinoma cell lines MCF-7 and MD-MBA-231 were used. The cytotoxicity was evaluated using MTT assay. Time-lapse microscopy and transmission electron microscopy were used to observe the morphological changes. Cell membrane integrity was assessed with propidium iodide (PI) uptake and lactate dehydrogenase (LDH) assay. Flow cytometry was used to measure reactive oxygen species (ROS) level and mitochondrial membrane potential (Δψm). A multimode microplate reader was used to analyze the intracellular ATP level. The changes in cytoskeletal system were investigated with Western blotting and immunostaining.
Results: Fluopsin C (0.5–8 μmol/L) reduced the cell viability in dose- and time-dependent manners. Its IC_{50} values in MCF-7 and MD-MBA-231 cells at 24 h were 0.9 and 1.03 μmol/L, respectively. Fluopsin C (2 μmol/L) induced oncosis in both the breast adenocarcinoma cells characterized by membrane blebbing and swelling, which was blocked by pretreatment with the pan-caspase inhibitor Z-VAD-fmk. In MCF-7 cells, fluopsin C caused PI uptake into the cells, significantly increased LDH release, induced cytoskeletal system degradation and ROS accumulation, decreased the intracellular ATP level and Δψm. Noticeably, fluopsin C exerted comparable cytotoxicity against the normal human hepatocytes (HL7702) and human mammary epithelial cells with the IC_{50} values at 24 h of 2.7 and 2.4 μmol/L, respectively.
Conclusion: Oncotic cell death was involved in the anticancer effects of fluopsin C on human breast adenocarcinoma cells *in vitro*. The hepatoxicity of fluopsin C should not be ignored.

Keywords: fluopsin C; *Pseudomonas jinanesis*; oncosis; human breast adenocarcinoma; membrane blebs

Acta Pharmacologica Sinica (2013) 34: 1093–1100; doi: 10.1038/aps.2013.44; published online 27 May 2013

Introduction

Apoptosis and oncosis, two major forms of cell death, have distinct morphological and biochemical features[1, 2]. Apoptosis is considered to be the major form of cell death in various physiological events. Apoptosis is characterized by the condensation of the cytoplasm and chromatin, DNA fragmentation, and cell fragmentation into apoptotic bodies, followed by the removal and degradation of the dying cells through phagocytosis[3]. In contrast, oncosis is a process of passive cell death related to energy depletion, leading to the impairment of cell membrane ionic pumps, the swelling of the cell, the formation of cell surface blebs, the condensation of mitochondria, and an increase in membrane permeability. Oncosis is the pattern of change in infarcts and zonal killing following chemical toxicity[4, 5].

Although the molecular mechanisms of apoptosis have been well characterized[6–8], a comprehensive picture depicting oncosis regulation is still lacking. Recently, there has been increasing interest in the mechanistic relationship between cell death *via* apoptosis and oncosis[2, 9]. Emerging evidence has suggested a complex interplay between these two cellular processes, which seem to have some common regulatory mechanisms. In addition, several regulators in the apoptotic pathway, such as reactive oxygen species (ROS), mitochondrial injury, calcium overload, and adenosine triphosphate (ATP) depletion, have been found to function as modulators of oncosis[1, 10].

Breast cancer is a prevalent disease and a leading cause of cancer death in women worldwide. Many treatments, such as chemotherapy, which is still the most effective clinical therapy, have been developed to improve prognosis and decrease the

# The two authors contributed equally to this work.
* To whom correspondence should be addressed.
E-mail xiali@sdu.edu.cn
Received 2012-12-23 Accepted 2013-03-12

risk of recurrent diseases[11, 12]. However, the development of novel therapeutic agents is greatly needed. The current study was undertaken to investigate the effects and mechanisms that underlie the anticancer activity of fluopsin C (Figure 1), an antibiotic isolated from *Pseudomonas jinanesis*.

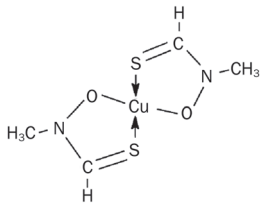

Figure 1. Chemical structure of fluopsin C.

Antibiotics are clinically important drugs for fighting tumor cells. Fluopsin C is an antibiotic that has been purified and isolated from *P fluorescens, Pseudomonas sp*, *P aeruginosa*, and *Streptomyces*[13, 14]. Previous studies demonstrated that fluopsin C exhibited strong antitumor, antibacterial, and antifungal properties[13–15]. However, the nature and characteristics of the cytotoxic effect and the mechanisms of fluopsin C-induced cell death remain to be elucidated. In the current study, fluopsin C was demonstrated to mediate its cytotoxicity via oncosis in the MCF-7 and MD-MBA-231 human breast cancer cell lines.

Materials and methods

Cell culture and reagents

Human breast adenocarcinoma (MCF-7 and MD-MBA-231) cell lines and a normal human hepatocyte cell line (HL7702) were obtained from the Shanghai Institute for Biological Sciences (SIBS), Chinese Academy of Sciences (China). Another normal cell line, HMLE, which was derived from normal human mammary epithelial cells immortalized with the catalytic subunit of telomerase and SV40 large-T and small-T antigens, was kindly provided by Dr Chang-jun ZHU (Shandong University). The MCF-7 and HL7702 cells were maintained in RPMI-1640 medium (Hyclone, Thermo Fisher Scientific, Beijing, China), and the MD-MBA-231 cells were cultured in modified DMEM (Gibco, Invitrogen Corporation, Grand Island, NY, USA). All media were supplemented with 10% heat-inactivated fetal bovine serum (TBD, Tianjin, China), 100 U/mL penicillin and 100 μg/mL streptomycin. The HMLE cells were cultured in serum-free mammary epithelial cell growth medium (Lonza, Allendale, NJ, USA). The cells were cultured in a humidified atmosphere of 5% CO_2 at 37 °C.

Purified (over 98% pure) fluopsin C was dissolved in dimethylsulfoxide (DMSO) as a 1 mmol/L stock solution at -20 °C and diluted according to experimental requirements. 3-(4,5-dimethylthiazol)-2,5-diphenyltetrazolium bromide (MTT) and 4′,6-diamidino-2-phenylindole (DAPI) were purchased from Sigma (USA). The caspase inhibitor Z-VAD-fmk (C1202) and JC-1 were purchased from the Beyotime Institute of Biotechnology, Haimen, China. All chemicals used in this study were commercial products of reagent grade.

Cytotoxicity analysis

The MTT assay is widely used to measure cell proliferation and cytotoxicity. Cells (4×10^3–5×10^3 per well) were seeded in 96-well culture plates. After incubation for 24 h, the cells were pretreated with or without the caspase inhibitor Z-VAD-fmk at the indicated concentrations 1 h prior to the administration of fluopsin C at various concentrations for the indicated times. Next, 20 μL of MTT (5 mg/mL) was added to each well for 4 h, and the resulting crystals were dissolved in DMSO. The optical density of each well was measured using a microplate reader (Bio-Rad 680) at 570 nm. Wells containing DMSO were used for control cell viability and represented 100% cell survival, and wells without cells were used for blanking the spectrophotometer. The cell viability ratio (%) was calculated as $(A_{570\ sample}-A_{570\ blank})/(A_{570\ control}-A_{570\ blank})\times100\%$. IC_{50} values for each cell line were evaluated as the dose of drug causing 50% absorbance reduction in comparison with DMSO-treated control cells. Each test was performed in triplicate.

Time-lapse microscopy analysis

MCF-7 and MD-MBA-231 cells grown on 35-mm glass-bottom microwell dishes (MatTek, Ashland, MA) were cultured with CO_2-independent medium (Gibco) containing 10% FBS overnight. After treatment with 2 μmol/L fluopsin C or 2 μmol/L fluopsin C plus Z-VAD-fmk, the dishes were rapidly covered with mineral oil (Sigma), transferred to a heated stage (37 °C) and observed with a live cell digital imaging system. Phase-contrast images of live cells were collected at 1-min intervals for 0–3 h, 5-min intervals for 4–6 h and 15-min intervals for 7–9 h with the live cell digital imaging system (PlanApo 409, NA 1.40). The movies were edited with Image Analysis software (*InVitro*, Media Cybernetics, USA).

Transmission electron microscopy

MCF-7 cells that were treated or untreated with 2 μmol/L fluopsin C were washed twice with PBS, fixed with 4% glutaraldehyde for 1 h at room temperature and centrifuged at 3000 r/min. Post-fixation was carried out in 0.15 mol/L phosphate buffer with 3% OsO_4 for 1 h, followed by a rapid wash in the same buffer. Next, the specimens were dehydrated with alcohol-water solutions of varying concentrations and 100% propylene oxide, respectively. Araldite embedding began with a 1:1 mixture of propylene oxide: araldite (*v/v*) for 1 h, followed by 1:3 mixtures overnight at room temperature. After an additional treatment in undiluted resin for 1 h, polymerization was performed at 60 °C for 3–4 d. Thin sections stained with 1% toluidine blue were mounted on copper grids. Grids were observed under a transmission electron microscope (JEM-1200EX, Japan) at 60 kV.

Propidium iodide (PI) uptake assay

The cell membrane integrity of fluopsin C-treated cells was assessed by monitoring the uptake of the fluorescent probe PI (Sigma, St Louis, Missouri, USA). PI is a membrane impairment nuclear stain that is used as an indicator for determining the cell membrane integrity[16]. To determine PI uptake, cells

were seeded in 24-well plates. After 24 h, cells were treated with 2 μmol/L fluopsin C (0–9 h) and incubated with PI (4 μg/mL) at 37 °C for 15 min in the dark. After being washed twice to remove unbound PI, the cells were observed under an inverted fluorescence microscope (Olympus IX71, Japan). Fluorescent images were recorded using a cooled CCD camera.

PI uptake was also examined through flow cytometry analysis. MCF-7 cells seeded in 6-well plates were treated with 2 μmol/L fluopsin C for 24 h and then collected and incubated with the PI staining solution (10 μg/mL) for 15 min in the dark. Cellular fluorescence was measured through flow cytometry.

Lactate dehydrogenase (LDH) assay

Plasma membrane integrity was also monitored by measuring LDH release into the medium. Cells were seeded in 96-well culture plates at a density of 1×10^6/mL for 24 h and then cultured in serum-free medium with fluopsin C 2 μmol/L for 0–9 h. LDH released into cell culture supernatants was detected using an LDH assay kit (Keygen Biotech Co, Ltd, Nanjing, China). As a control for maximum LDH release, cells were treated with 1% Triton-X-100 (Sigma) in RPMI-1640 medium for 10 min (100% release). The absorbance was measured using a microplate reader (Bio-rad 680) at 450 nm.

Cell content leakage assay

Cells were treated with 2 μmol/L fluopsin C for different times (0–9 h). The amount of intracellular contents that leaked from cells was estimated by analyzing the supernatants. The $OD_{260\,nm}$ was recorded using a Bio-Rad SmartSpec plus.

Immunostaining and fluorescence microscopy

Cells were seeded onto cover slips in 24-well plates and incubated with 2 μmol/L fluopsin C for different times (0–6 h). The cells were washed with PBS twice and fixed in methanol/acetone (1:1) for 5 min before being washed twice with cold PBS. The cells were incubated in 3% goat serum in PBS with 0.1% Triton X-100 for 20 min at room temperature. The cells were then incubated with primary antibodies against α-tubulin and β-actin (Sigma, Co, USA) for 2 h at room temperature. Cells were washed and incubated with anti-rabbit IgG-FITC (1:200) and anti-mouse IgG-Alexa Fluor 555 (1:250) for 1–2 h. The nuclei were counterstained with 2 μg/mL DAPI for 10 min at room temperature. After being washed three times, the cover slips containing cells were mounted onto glass slides using FluoroGuard (Bio-Rad, Richmond, CA) and imaged using a fluorescence microscope[17] .

Western blotting analysis

Total cell lysates were analyzed with Western blotting. Samples were boiled in 1×Laemmli buffer, subjected to 12% SDS-polyacrylamide gel electrophoresis and transferred to nitrocellulose membranes. The membrane was washed in distilled water and blocked with 5% non-fat milk in TBS-T buffer [10 mmol/L Tris-HCl, 150 mmol/L NaCl, and 0.05% (*v/v*) Tween-20, pH 7.8] for at least 1 h at room temperature. After a short wash in TBS-T buffer, the membranes were incubated with monoclonal antibodies specific for β-actin and α-tubulin (Sigma, Co, USA) for at least 2 h at room temperature or overnight at 4 °C. The membranes were then incubated with secondary HRP-conjugated goat anti-mouse IgG or anti-rabbit IgG (diluted 1:1000; Santa Cruz Biotechnology, Inc, USA). Proteins on the membranes were visualized using the enhanced chemiluminescence detection system (ECL®, Amersham Biosciences).

Intracellular ATP measurement

Cells were grown in 96-well plates and incubated with 2 μmol/L fluopsin C for 0–9 h. Intracellular ATP levels were determined using an ATP determination kit (Beyotime institute of Biotechnology) according to the manufacturer's protocol. The entire cell population, including any floating cells, was assayed. Luminescence was measured using a Mithras LB 940 multimode microplate reader (Germany Berthold).

ROS measurement

Changes in intracellular ROS levels were quantified by measuring the oxidative conversion of the cell-permeable nonfluorescent dye 2′,7′-dichlorofluorescein diacetate (DCFH-DA) into fluorescent dichlorofluorescein (DCF). In the presence of ROS, DCFH reacts with ROS to form the fluorescent product DCF, which is trapped inside the cells. To detect fluopsin C-induced intracellular ROS accumulation, MCF-7 cells grown in 6-well plates were rinsed once with PBS and then treated with 2 μmol/L fluopsin C at 37 °C for 0–6 h. After incubation, the culture medium was removed, and the cells were washed three times with PBS. The cells were incubated with DCFH-DA (10 μmol/L, Beyotime Institute of Biotechnology, China) at 37 °C for 30 min. Cellular fluorescence was measured through flow cytometry with a FACS-SCAN apparatus (Becton Dickinson, USA). Decreased values compared to the control were considered to represent decreases in intracellular ROS levels.

Mitochondrial membrane potential measurement

Mitochondrial membrane permeabilization involves the formation of pores or channels that lead to the dissipation of the mitochondrial membrane potential ($\Delta\psi_m$)[18]. JC-1, a lipophilic, cationic fluorescent probe, was used to measure the $\Delta\psi_m$ of MCF-7 cells according to the manufacturer's instruction. Cells were exposed to fluopsin C 2 μmol/L for 0–9 h and incubated with the JC-1 staining solution (5 μg/mL) for 30 min at 37 °C. The cells were then rinsed twice with JC-1 staining buffer. The fluorescence intensities of both JC-1 monomers (FL1-H) and aggregates (FL2-H) were detected through flow cytometry. The data were analyzed using Cell Quest software (Becton Dickinson, USA). The $\Delta\psi_m$ for each treatment group was calculated as the ratio of red (aggregates) to green (monomers) fluorescence.

Statistical analysis

All experiments were repeated at least in triplicate. Statistical analysis was performed using an analysis of variance

(ANOVA) followed by Turkey's *t*-test. *P*-values less than 0.05 were considered to be statistically significant.

Results

Fluopsin C cytotoxicity

The cytotoxic effects of fluopsin C on human breast adenocarcinoma cells and normal cells (HL7702 and HMLE) were determined *via* MTT assay. As shown in Figure 2, cells treated with fluopsin C (0.5 to 8 μmol/L) for different times (6, 12, and 24 h) exhibited a decrease in viability in a dose- and time-dependent manner. The IC_{50} values were 2.9, 1.6, and 0.9 μmol/L for MCF-7 cells and 2.8, 1.9, and 1.03 μmol/L for MD-MBA-231 cells treated with fluopsin C for 6, 12, and 24 h, respectively. However, cytotoxicity against human hepatocyte cells (HL7702) and human mammary epithelial (HMLE) cells was also observed, although the IC_{50} was higher for HL7702 and HMLE cells than for the breast adenocarcinoma cells (the IC_{50} values for HL7702 were 7.2, 4.4, and 2.7 μmol/L at 6, 12, and 24 h; the IC_{50} values for HMLE were 9.7, 4.8, and 2.4 μmol/L at 6, 12, and 24 h, respectively), suggesting the necessity of investigating the anticancer activity of fluopsin C and considering its toxicity in future clinical use and drug development.

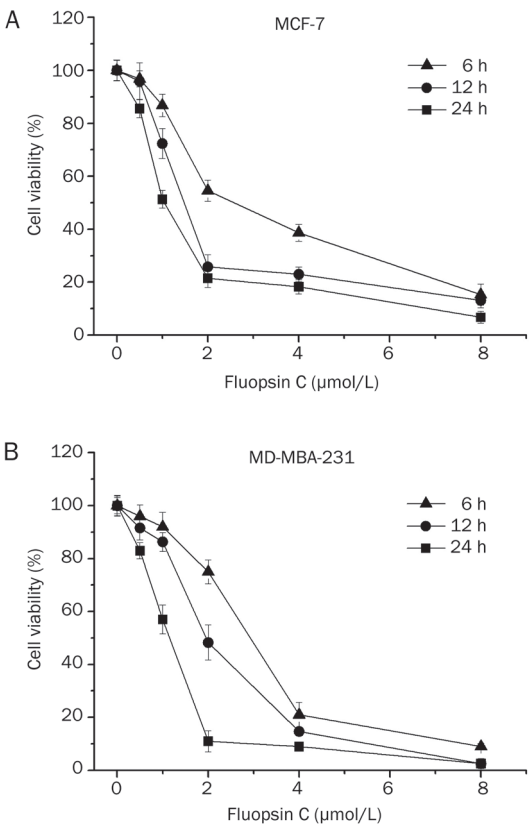

Figure 2. Cytotoxicity of fluopsin C in MCF-7 and MD-MBA-231 cells. Dose- and time-dependent cytotoxic effects of fluopsin C on (A) MCF-7 cells and (B) MD-MBA-231 cells. Cell viability was determined relative to the population of untreated control cells at the same time point. The data are expressed as the mean±SD (% cell viability) of triplicate experiments.

Fluopsin C induced oncosis in MCF-7 and MD-MBA-231 cells

Time-lapse microscopy was performed to observe morphological changes during the fluopsin C-induced cell death of breast cancer cells MCF-7 and MD-MBA-231. Cells treated with fluopsin C showed cell swelling and membrane surface blebs. Figure 3 shows that the blebs in MD-MBA-231 and MCF-7 cells formed as early as 1 h post-treatment with fluopsin C, and the blebs lasted for 9 h in these two cells. However, cell swelling lasted longer, which led to membrane disruption. These results indicated that fluopsin C exhibited morphologic oncotic features and induced changes of the plasma membrane.

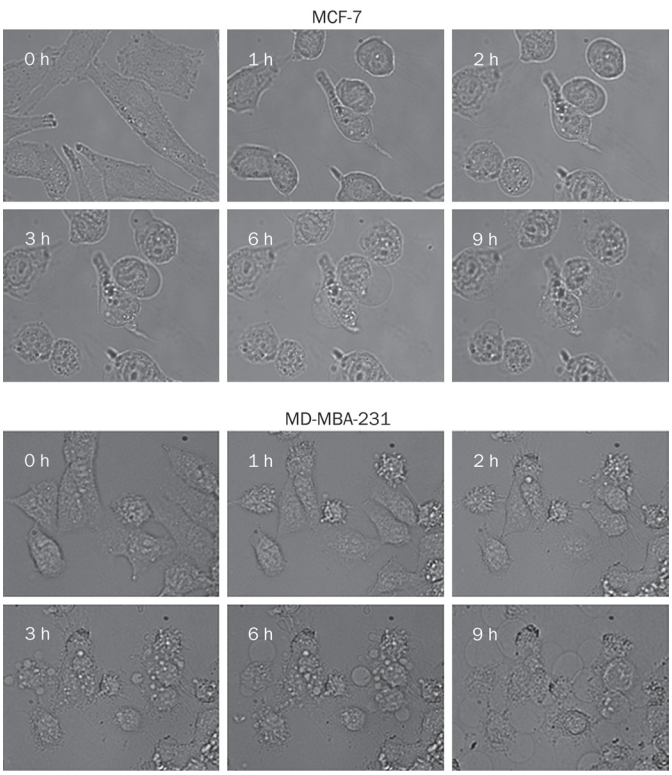

Figure 3. Time-lapse analysis of cell membrane bleb formation induced by 2 μmol/L fluopsin C in MCF-7 and MD-MBA-231 cells.

The ultrastructural details of fluopsin C-treated cells were further examined at 6 h and 12 h post-treatment with transmission electron microscopy (TEM) (Figure 4A). Cytoplasmic and nuclear swelling was apparent at 3 h after treatment with fluopsin C compared with control cells. The nucleus was filled with dispersed chromatin. The plasma membrane was intact, but vacuolization was observed in all membrane-bound organelles. After 9 h of incubation, the plasma membrane was destroyed, and vacuolization of the perinuclear cisterna, endoplasmic reticulum and mitochondria was observed. The entire cell exhibited low electron density resulting from failure of the ionic pumps in the plasma membrane. Most of the treated cells lacked pseudopodia, which were common in control cells. These features were distinct from apoptotic cells. These TEM

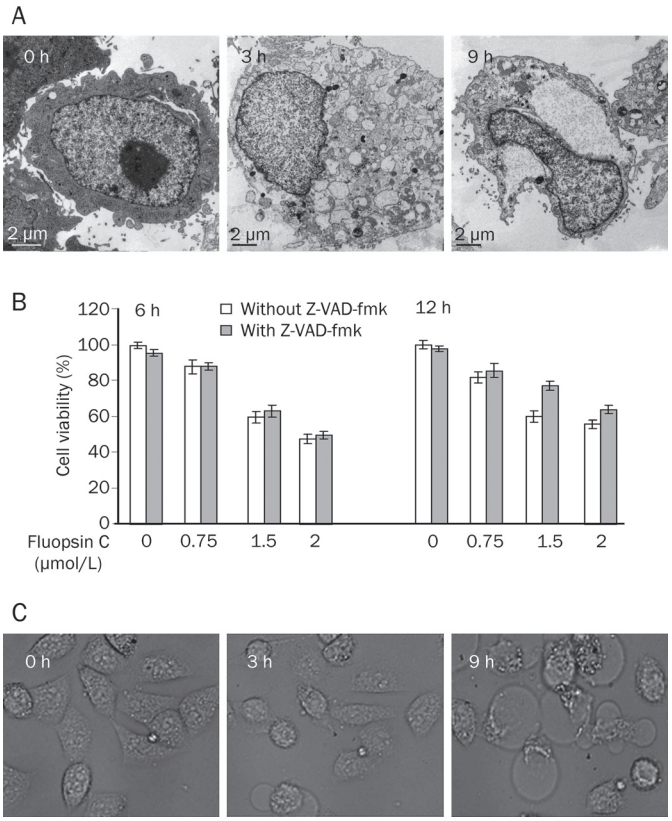

Figure 4. (A) Electron micrographs of fluopsin C-treated MCF-7 cells. (B) Effects of Z-VAD-fmk on the fluopsin C-induced reduction of cell viability. Cell viability was determined with the MTT assay after treatment with various concentrations of fluopsin C for 6–12 h in the absence or presence of Z-VAD-fmk (50 μmol/L, pretreated for 1 h). (C) Morphological changes in MCF-7 cells treated with 2 μmol/L fluopsin C for 9 h in the presence of Z-VAD-fmk (50 μmol/L, pretreated for 1 h) were observed using time-lapse analysis.

studies enabled us to demonstrate that fluopsin C-induced cell death in MCF-7 cells exhibited features of oncosis.

Fluopsin C-induced oncosis is not blocked by the caspase inhibitor Z-VAD-fmk

The fluopsin C-induced cell death pathway was further investigated using the pan-caspase inhibitor Z-VAD-fmk. MCF-7 cells were pretreated with the pan-caspase inhibitor Z-VAD-fmk (50 μmol/L) for 1 h and then treated with fluopsin C for 6–12 h. Treatment with Z-VAD-fmk up to 50 μmol/L was only slightly toxic, and fluopsin C-induced cell death was not inhibited by Z-VAD-fmk (Figure 4B). In contrast to apoptosis, oncosis does not involve caspases[19]. As depicted in Figure 4B, pretreatment with Z-VAD-fmk at 50 μmol/L did not exhibit an inhibitory effect on the cell swelling or vacuolization induced by fluopsin C. These results suggested that fluopsin C-induced cell death was independent of the caspase pathway.

To confirm whether Z-VAD-fmk affected fluopsin C-induced cell death, we performed a time-lapse microscopy experiment to observe the morphological changes after treatment with fluopsin C plus Z-VAD-fmk in MCF-7 cells. Pretreatment with Z-VAD-fmk did not change the fluopsin C-induced cell morphologic characteristics in MCF-7 cells (Figure 4C).

Fluopsin C disrupted the cell membrane integrity

The integrity of the cell membrane was determined by PI uptake (DNA intercalating fluorescent dye)[16]. The cells were stained with PI and subsequently analyzed using fluorescence microscopy and flow cytometry. Figure 5 show the unstained control cells and cells treated with fluopsin C, which were stained with PI, indicating a disrupted cell membrane.

Further experiments were conducted to determine whether the integrity of the cell membrane was disrupted by fluopsin C. LDH and cytoplasmic content leakage into the culture medium are characteristic indicators of plasma membrane disruption[20]. First, plasma membrane integrity was monitored by measuring the release of LDH into the incubation medium. The LDH release of MCF-7 cells increased after 90 min of treatment with 2 μmol/L fluopsin C and peaked at approximately 9 h (Figure 6A).

The leakage of cytoplasmic contents was assessed by measuring the *OD* at 260 nm. After 6 h of fluopsin C treatment, the $OD_{260\ nm}$ of filtrates from MCF-7 cell suspensions was significantly increased (Figure 6B).

Fluopsin C destroyed the cell skeleton

Several studies have suggested that surface bleb formation and plasma membrane integrity are related to alterations of the cytoskeletal network[20–22]. In the current study, immunocytochemical investigations revealed changes in the cytoskeletal network of fluopsin C-exposed cells. As shown in Figure 7A, the loss of microtubules and actin microfilaments was observed in fluopsin C-treated cells. A Western blot assay was used to detect the related proteins β-actin and α-tubulin. Figure 7B shows that immunoblotting of the treated cell lysates displayed an obvious decrease in both proteins. Fluopsin C-induced plasma membrane blebs may be related to the destruction of microtubules and actin in cells.

Fluopsin C induced ATP depletion, ROS generation and $\Delta\psi_m$ collapse

Several studies have suggested that ROS and cellular ATP play a pivotal role in determining whether cell death is apoptotic or oncotic[2, 23, 24]. Figure 8A shows that the cellular ATP content of MCF-7 cells in the presence and absence of fluopsin C was significantly decreased.

The effect of fluopsin C on ROS generation was determined. MCF-7 cells treated with or without fluopsin C were incubated with DCFH-DA for 30 min. DCF-derived fluorescence was then measured as an index of ROS accumulation. Flow cytometric assay showed a greater accumulation of ROS in fluopsin C-treated MCF-7 cells compared with untreated MCF-7 cells (Figure 8B).

In addition, the $\Delta\psi_m$ of MCF-7 cells was quantified via flow cytometry using a JC-1 cationic dye. Figure 8C shows that the

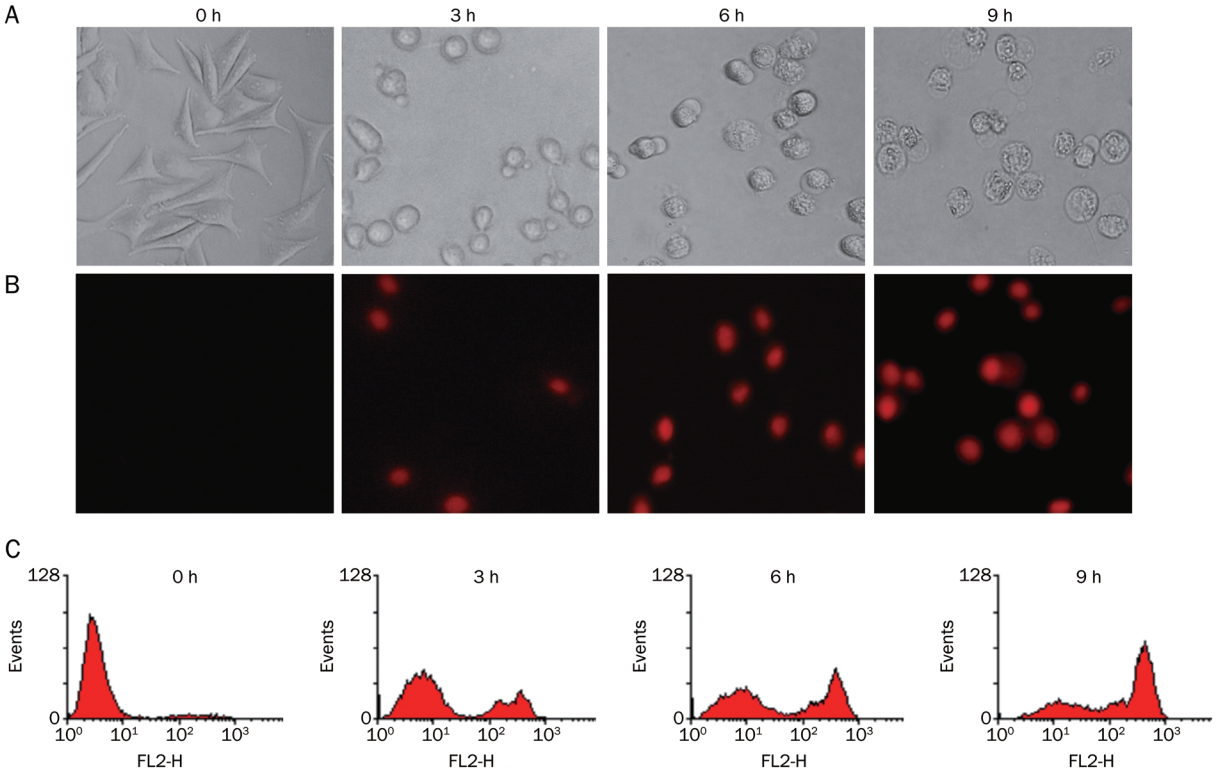

Figure 5. Morphological changes and PI uptake in MCF-7 cells. (A) Morphological changes after 2 μmol/L fluopsin C treatment observed under an inverted light microscope and recorded with an automatic digital charge-coupled device camera (Magnification ×100). (B) PI uptake analyzed under a fluorescent microscope (Magnification ×100). (C) PI uptake analyzed by flow cytometric analysis.

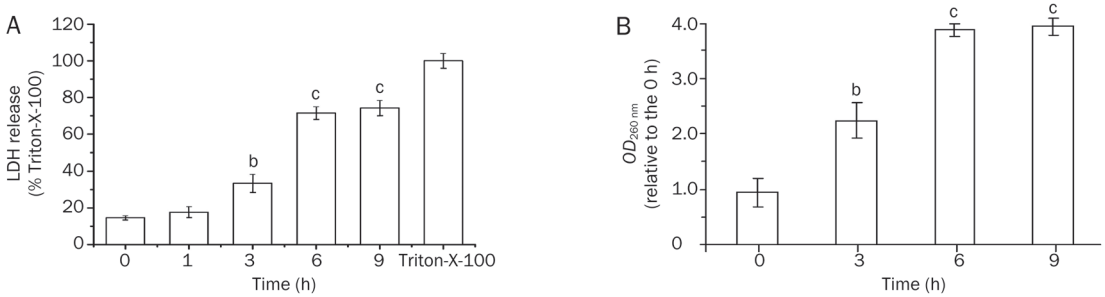

Figure 6. (A) LDH release from MCF-7 cells subjected to 2 μmol/L fluopsin C treatment. MCF-7 cells were treated with 1% Triton-X-100 (Sigma) in RPMI-1640 medium for 10 min as the 100% LDH release control. $^{b}P<0.05$, $^{c}P<0.01$ *vs* the control (0 h). (B) Time-dependent release of cellular materials assessed at 260 nm from MCF-7 cells. The $OD_{260\ nm}$ of MCF-7 cells without fluopsin C treatment was set at 1.0. Data points represent the mean and standard deviation of three experiments. $^{b}P<0.05$, $^{c}P<0.01$ *vs* the control (0 h). The data are expressed as the mean±SD from triplicate experiments.

$\Delta\psi_m$ was significantly decreased in a time-dependent manner in fluopsin C-treated cells.

Discussion

Oncosis, derived from the Greek word "swelling", is a cell death mode with distinct morphological and biochemical features. In the current study, fluopsin C-induced oncotic cell death of breast cancer cells was demonstrated for the first time, and a damaged cytoskeleton and mitochondria were shown to be involved.

In the current study, fluopsin C significantly reduced the viability of breast cancer cells in a concentration- and time-dependent manner. Furthermore, the examination of the morphological changes of fluopsin C-treated MCF-7 and MD-MBA-231 cells via time-lapse microscopy revealed cellular features characteristic of oncotic death, such as extensive cytoplasmic vacuolization, cellular and organelle swelling, and rupture of the plasma membrane, typical features of oncosis[4, 5].

MCF-7 cells were employed to further explore the action

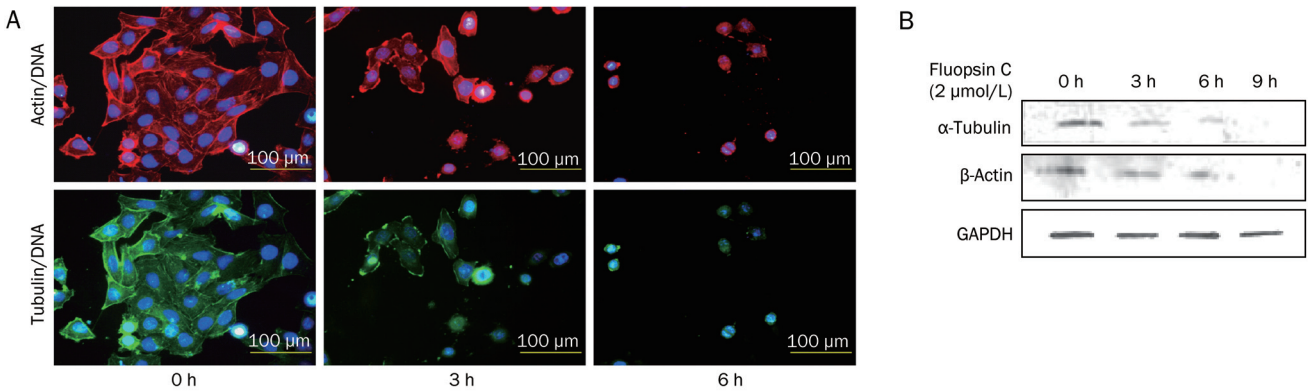

Figure 7. (A) Effects of fluopsin C on actin and microtubule distribution in MCF-7 cells analyzed under a fluorescent microscope (Magnification ×100). (B) Expression levels of β-actin and α-tubulin in MCF-7 cells treated with or without fluopsin C through Western blotting.

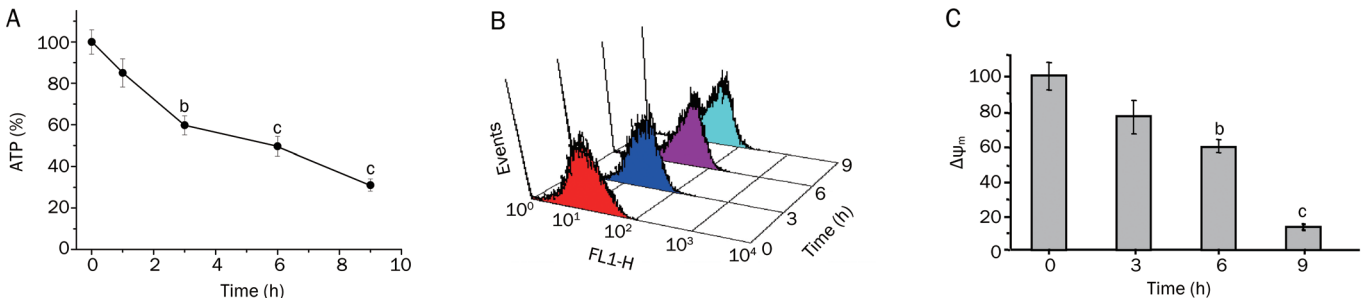

Figure 8. (A) The levels of intracellular ATP decreased after treatment with fluopsin C in a time-dependent manner. The ATP level in MCF-7 cells without fluopsin C treatment was set as 100%. $^{b}P<0.05$, $^{c}P<0.01$ *vs* the control (0 h). (B) Fluopsin C treatment led to the accumulation of intracellular ROS in MCF-7 cells, as assessed with flow cytometric analysis. The cells were treated with 2 μmol/L fluopsin C for 0 h to 9 h. ROS accumulation was quantified by measuring DCF-derived fluorescence with flow cytometry after incubating the cells with DCFH-DA for 30 min. (C) Fluopsin C induced the loss of $\Delta\psi_m$, as shown by flow cytometry. $^{b}P<0.05$, $^{c}P<0.01$ *vs* the control (0 h). The $\Delta\psi_m$ in MCF-7 cells without fluopsin C treatment was set as 100%.

and mechanisms of fluopsin C-induced cell oncosis. Plasma membrane rupture is also a cellular feature of oncotic death. The results of PI staining, LDH release into the medium, and 260 nm absorbing material release showed an increase in plasma membrane permeability during fluopsin C-mediated oncosis.

Apoptosis and oncosis share certain mechanisms and alterations, such as the loss of mitochondrial permeability and membrane potential, and the cell fate is mostly attributed to the intensity and duration of the death signal and the cell's genetic and metabolic status. Mitochondria have long been proposed as central players in oncotic cell death because they are the center of both ATP and ROS synthesis[25, 26]. The level of ATP has been suggested to be another key determinant of whether cells undergo apoptosis or oncosis. Apoptosis is an active, early-stage energy-dependent process that requires ATP to initiate the molecular cascade, whereas oncosis is an excessive ATP depletion process[27]. The intracellular ATP level of fluopsin C-treated MCF-7 cells at 3 h was depleted to less than 35% of the control, which confirmed that fluopsin C could induce oncosis in MCF-7 cells rather than apoptosis. Several investigators have shown that cells in an aerobic environment are constantly generating ROS[23, 24]. Because the physiologic levels of ROS can serve as signaling molecules to regulate transcription, excessive ROS production leads to oxidative stress, damage to intracellular molecules and organelles, and, ultimately, cell death. In the current study, fluopsin C-induced oncosis in MCF-7 cells was confirmed to be associated with enhanced ROS generation, and the current data also indicated that fluopsin C caused the loss of the $\Delta\psi_m$ in MCF-7 cells. ATP depletion and increased ROS could be the result of mitochondrial depolarization during fluopsin C-induced cell death in MCF-7 cells, which causes the collapse of the electrical gradient across the mitochondrial inner membrane.

The cytoskeleton has been shown to be involved in oncosis and plasma membrane permeability[20, 21, 28]. The depletion of cytoskeleton-associated proteins can break the membrane cytoskeleton linkage and decrease the physical support of the basal plasma membrane, leading to bleb formation and increased membrane permeability. In the present study, immunostaining and immunoblotting were used to observe changes in the levels of cytoskeleton-associated proteins β-actin and α-tubulin in fluopsin C-treated MCF-7 cells. Fluopsin C led to a significant decrease in β-actin and α-tubulin protein levels in a time-dependent manner.

Overall, these results suggest that fluopsin C induced breast

cancer cell death through a process involving cell swelling, membrane surface blebs, loss of membrane integrity, nuclear cell morphology different from apoptosis, and LDH and cytoplasm content release, which are classical signs of oncosis. Moreover, ROS generation, cellular ATP content depletion, and loss of $\Delta\psi_m$ was involved in fluopsin C-induced oncosis in breast tumor cells. Fluopsin C destroyed the cytoskeleton, including the microfilament and microtubule network, and decreased β-actin and α-tubulin protein levels in a time-dependent manner. However, the precise molecular mechanism by which fluopsin C induced oncotic death remains unclear. Further studies are warranted, and the hepatoxicity of fluopsin C should not be ignored.

Acknowledgements

This work was supported by grants from the National Natural Science Foundation of China (No 81273532) and the Shandong Provincial Natural Science Foundation (No ZR2011HQ028).

Author contribution

Prof Xia LI designed the research and revised the manuscript; Li-sha MA and Chang-you JIANG conducted the research, analyzed the data and wrote the paper; Min CUI, Rong LU, Shan-shan LIU, Bei-bei ZHENG, and Lin LI helped with portions of the research.

Supplementary information

Supplementary information is available at the Acta Pharmacologica Sinica website. Supplementary materials related to this article can be found online as Movie 1 and Movie 2.

References

1 Majno G, Joris I. Apoptosis, oncosis, and necrosis. An overview of cell death. Am J Pathol 1995; 146: 3–15.
2 Van Cruchten S, Van Den Broeck W. Morphological and biochemical aspects of apoptosis, oncosis and necrosis. Anat Histol Embryol 2002; 31: 214–23.
3 Carson DA, Ribeiro JM. Apoptosis and disease. Lancet 1993; 341: 1251–4.
4 Fu D, Tian L, Peng Z, Deng W, Yuan J, Ma D, *et al*. Overexpression of CHMP6 induces cellular oncosis and apoptosis in HeLa cells. Biosci Biotechnol Biochem 2009; 73: 494–501.
5 Roque-Navarro L, Chakrabandhu K, de Leon J, Rodriguez S, Toledo C, Carr A, *et al*. Anti-ganglioside antibody-induced tumor cell death by loss of membrane integrity. Mol Cancer Ther 2008; 7: 2033–41.
6 Fadeel B, Orrenius S. Apoptosis: a basic biological phenomenon with wide-ranging implications in human disease. J Intern Med 2005; 258: 479–517.
7 Green DR, Reed JC. Mitochondria and apoptosis. Science 1998; 281: 1309–12.
8 Li X, Wu WK, Sun B, Cui M, Liu S, Gao J, *et al*. Dihydroptychantol A, a macrocyclic bisbibenzyl derivative, induces autophagy and following apoptosis associated with p53 pathway in human osteosarcoma U2OS cells. Toxicol Appl Pharmacol 2011; 251: 146–54.
9 Moriguchi A, Otani H, Yoshioka K, Shimazu T, Fujita M, Okazaki T, *et al*. Inhibition of contractile activity during postconditioning enhances cardioprotection by restoring sarcolemmal dystrophin through phosphatidylinositol 3-kinase. Circ J 2010; 74: 2393–402.
10 Buja LM. Myocardial ischemia and reperfusion injury. Cardiovasc Pathol 2005; 14: 170–5.
11 Espinosa E, Vara JA, Redondo A, Sanchez JJ, Hardisson D, Zamora P, *et al*. Breast cancer prognosis determined by gene expression profiling: a quantitative reverse transcriptase polymerase chain reaction study. J Clin Oncol 2005; 23: 7278–85.
12 Gast MC, Schellens JH, Beijnen JH. Clinical proteomics in breast cancer: a review. Breast Cancer Res Treat 2009; 116: 17–29.
13 Otsuka H, Niwayama S, Tanaka H, Take T, Uchiyama T. An antitumor antibiotic, No 4601 from *Streptomyces*, identical with YC 73 of *Pseudomonas* origin. J Antibiot 1972; 25: 369–70.
14 Ito S, Inuzuka K, Suzuki T. New antibiotics produced by bacteria grown on *n*–paraffin (mixture of C12, C13, and C14 fractions). J Antibiot 1970; 23: 542–5.
15 Shirahata K, Deguchi T, Hayashi T, Matsubara I, Suzuki T. The structures of fluopsins C and F. J Antibiot 1970; 23: 546.
16 Wang KR, Yan JX, Zhang BZ, Song JJ, Jia PF, Wang R. Novel mode of action of polybia-MPI, a novel antimicrobial peptide, in multi-drug resistant leukemic cells. Cancer Lett 2009; 278: 65–72
17 Li X, Zhao Y, Wu WK, Liu S, Cui M, Lou H. Solamargine induces apoptosis associated with p53 transcription-dependent and transcription-independent pathways in human osteosarcoma U2OS cells. Life Sci 2011; 88: 314–21.
18 Kroemer G, Galluzzi L, Brenner C. Mitochondrial membrane permeabilization in cell death. Physiol Rev 2007; 87: 99–163.
19 Kroemer G, Galluzzi L, Vandenabeele P, Abrams J, Alnemri ES, Baehrecke EH, *et al*. Classification of cell death: recommendations of the nomenclature committee on cell death 2009. Cell Death Differ 2009; 16: 3–11.
20 Sun L, Zhao Y, Yuan H, Li X, Cheng A, Lou H. Solamargine, a steroidal alkaloid glycoside, induces oncosis in human K562 leukemia and squamous cell carcinoma KB cells. Cancer Chemother Pharmacol 2011; 67: 813–21.
21 Malorni W, Iosi F, Mirabelli F, Bellomo G. Cytoskeleton as a target in menadione-induced oxidative stress in cultured mammalian cells: alterations underlying surface bleb formation. Chem Biol Interact 1991; 80: 217–36.
22 Neisch AL, Speck O, Stronach B, Fehon RG. Rho1 regulates apoptosis *via* activation of the JNK signaling pathway at the plasma membrane. J Cell Biol 2010; 189: 311–23.
23 Goldmann O, Sastalla I, Wos–Oxley M, Rohde M, Medina E. *Streptococcus pyogenes* induces oncosis in macrophages through the activation of an inflammatory programmed cell death pathway. Cell Microbiol 2009; 11: 138–55.
24 Cao X, Zhang Y, Zou L, Xiao H, Chu Y, Chu X. Persistent oxygen-glucose deprivation induces astrocytic death through two different pathways and calpain-mediated proteolysis of cytoskeletal proteins during astrocytic oncosis. Neurosci Lett 2010; 479: 118–22.
25 Jennings RB, Reimer KA. Lethal myocardial ischemic injury. Am J Pathol 1981; 102: 241–55.
26 Halestrap A. A pore way to die. Nature 2005; 434: 578–9.
27 Kalischuk LD, Inglis GD, Buret AG. Strain-dependent induction of epithelial cell oncosis by *Campylobacter jejuni* is correlated with invasion ability and is independent of cytolethal distending toxin. Microbiology 2007; 153: 2952–63.
28 Liu X, Schnellmann RG. Calpain mediates progressive plasma membrane permeability and proteolysis of cytoskeleton-associated paxillin, talin, and vinculin during renal cell death. J Pharmacol Exp Ther 2003; 304: 63–70.